



Cite this: DOI: 10.1039/d0sm00566e

Detection of sub-degree angular fluctuations of the local cell membrane slope using optical tweezers

 Rahul Vaippully,^a Vaibavi Ramanujan,^b Manoj Gopalakrishnan,^a Saumendra Bajpai^b and Basudev Roy *^a

Normal thermal fluctuations of the cell membrane have been studied extensively using high resolution microscopy and focused light, particularly at the peripheral regions of a cell. We use a single probe particle attached non-specifically to the cell-membrane to determine that the power spectral density is proportional to (frequency)^{-5/3} in the range of 5 Hz to 1 kHz. We also use a new technique to simultaneously ascertain the slope fluctuations of the membrane by relying upon the determination of pitch motion of the birefringent probe particle trapped in linearly polarized optical tweezers. In the process, we also develop the technique to identify pitch rotation to a high resolution using optical tweezers. We find that the power spectrum of slope fluctuations is proportional to (frequency)⁻¹, which we also explain theoretically. We find that we can extract parameters like bending rigidity directly from the coefficient of the power spectrum particularly at high frequencies, instead of being convoluted with other parameters, thereby improving the accuracy of estimation. We anticipate this technique for determination of the pitch angle in spherical particles to high resolution as a starting point for many interesting studies using the optical tweezers.

 Received 1st April 2020,
 Accepted 22nd July 2020

DOI: 10.1039/d0sm00566e

rsc.li/soft-matter-journal

Rheology of the cell membrane assumes significance in cell migration, adhesion, differentiation and development,^{1–4} not to mention, also in probing the health of the cell. It is directly influenced in diseases like malaria⁵ and sickle cell anaemia.⁶ Further, the cancer cells are softer and more elastic compared to healthy ones to help in intravasation,⁷ when trying to get into the blood vessels and spread through the body. The exact mechanism by which it changes the elasticity is however not known.⁸ In view of all these facets, study of membrane facets and the subsequent response to external perturbations attains enormous importance.

Membrane fluctuations are inherent to many membrane processes, like ion-pump functioning, vesicle budding and trafficking^{9–11} in living cells. Our knowledge of the mechanisms of the membrane processes shall be significantly improved while learning about the nature of active fluctuations^{12,13} in membranes.

Typically, the normal membrane fluctuations have been studied to ascertain the rheological parameters of the living cells.¹³ These fluctuations are powered by thermal energy as

well as ATP dependent processes. The temporal range of such fluctuations is quite broad, starting from slow (10 s) actin waves that drive large wavelength fluctuations (100 nm to 10 μm) at cell edges and basal membrane,^{14–16} to relatively smaller amplitude ones (5 to 50 nm) which appear at the basal membrane^{17,18} and are mainly thermal in nature. Fluctuations of the basal membrane, as opposed to the cell edges have not been explored much due to requirements of high resolution. We use a new technique where we place a particle on top of a cell membrane at locations away from the cell edges to find the normal fluctuations after ensuring non-specific binding. This does not require proximity to a second surface as the interference is between the unscattered light in photonic force microscopy with that of the scattered light from the particle,^{19–21} and thus the unconfined free surface of the cell can also be probed.

Here, we also introduce a hitherto new concept, that of membrane local slope fluctuations, to study the parameters. To perform such a measurement, we show how the pitch-rotation angle²² of a spherical particle attached to the membrane can be ascertained at high resolution in optical tweezers to add additional parameters that can greatly improve the accuracy. The normal thermal fluctuations of the cell membrane have been regularly used to ascertain the properties of the membrane like the bending rigidity from the power spectral density when performed with techniques like membrane flickering.^{23,24} However,

^a Department of Physics, Indian Institute of Technology Madras, Chennai, 600036, India. E-mail: basudev@iitm.ac.in

^b Department of Applied Mechanics, Indian Institute of Technology Madras, Chennai, 600036, India

the power law fit to the normal thermal fluctuations particularly at high frequencies leads to a coefficient which includes both the bending rigidity and the cytoplasmic viscosity as multiplicative factors. Estimates to bending rigidity are then made after numerical integration and estimating the coefficients in the different regimes of low frequency, intermediate frequency and high frequency. Thus the error in estimation of bending rigidity is high. In our technique, the slope fluctuations, which we introduced for the first time, directly gives the estimate for the bending rigidity from the coefficient of the power law fit to the PSD at high frequency. Combining the PSD for normal fluctuations and the slope fluctuations, the bending rigidity and the cytoplasmic viscosity can be accurately ascertained with lower error bars than from the normal fluctuations alone. During the process of ascertaining the slope fluctuations, we show, for the first time, how to find the pitch-rotational angle to high accuracy using optical tweezers. The technique also does not require complicated contact based methods.²⁴ The bending rigidity has recently been shown to be correlated to membrane viscosity,²³ another important membrane parameter.

1 Theory

The pitch signal is given as the difference-in-halves signal of the light scattered by the birefringent particle placed inside crossed polarizers,²² and can also extend to particles trapped in optical tweezers. The pitch signal is linearly proportional to the difference-in-halves signal. The power spectrum due to pitch Brownian motion is given as follows, in consistency with the conventional power spectra in optical tweezers.²⁵

$$\text{PSD} = \frac{A}{f^2 + B} \quad (1)$$

The calibration factor β and the optical trap stiffness κ_1 are given as

$$\kappa_1 = 2\pi\gamma\sqrt{B} \quad (2)$$

$$\beta = \sqrt{\frac{k_B T}{\gamma A}} \quad (3)$$

where, γ is the drag coefficient of the particle close to the surface of the membrane. The γ of the pitch rotation close to a surface relates to the drag coefficient away from surface γ_0 by the following relation.²⁶

$$\gamma = \frac{\gamma_0}{1 - (5/16)(a/s)^3 + (15/256)(a/s)^6} \quad (4)$$

where, a is the radius of the particle and s is the separation between the center of the particle and the surface.

Further, following the Wiener–Khinchin theorem, the power spectral density (PSD) of membrane height fluctuations is given by^{27,28}

$$\text{PSD}_z = \int dte^{i\omega t} \int \frac{d^2\mathbf{q}d^2\mathbf{q}'}{(2\pi)^4} \langle h_{\mathbf{q}}(0)h_{\mathbf{q}'}(t) \rangle \quad (5)$$

where $h_{\mathbf{q}}(t) = \int d^2\mathbf{r}e^{i\mathbf{q}\cdot\mathbf{r}}h(\mathbf{r},t)$ is the Fourier transform of the height fluctuation, whose auto-correlation is

$$\langle h_{\mathbf{q}}(0)h_{\mathbf{q}'}(t) \rangle = 4\pi^2 F(q)\delta(\mathbf{q} + \mathbf{q}')e^{-\omega_q t} \quad (6)$$

where

$$F(q) = \frac{k_B T}{\kappa q^4 + \sigma q^2} \quad (7)$$

from equipartition theorem, where κ is the bending modulus and σ is the surface tension of the membrane. Assuming an impermeable, flat cell membrane which separates two fluids of mean viscosity η , the wavelength relaxation rate ω_q is given by^{29–31}

$$\omega_q = \frac{\kappa q^4 + \sigma q^2}{4\eta q} \quad (8)$$

After using (6) in (5), and switching to plane polar coordinates, it follows that

$$\text{PSD}_z = \frac{1}{\pi} \int_{q_{\min}}^{q_{\max}} dq q F(q) \frac{\omega_q}{\omega_q^2 + \omega^2} \quad (9)$$

If we consider the cell has an infinite membrane with a point like detection area, $q_{\min} = 0$ and $q_{\max} = \infty$ in (3). Next, after using (7) and (8) in (3), it follows that the Z-power spectral density of a particle stuck on the membrane is

$$\text{PSD}_z = \frac{4\eta k_B T}{\pi} \int_0^{\infty} \frac{dq}{(\kappa q^3 + \sigma q)^2 + (4\eta\omega)^2} \quad (10)$$

This integral cannot be solved analytically in the present form, and only numerical estimates can be made. Thus, approximations are considered. In the low frequency limit, *i.e.*, when $\omega \rightarrow 0$, it can be shown that

$$\text{PSD}_z \sim \frac{k_B T}{2\sigma\omega} \quad (\omega \rightarrow 0), \quad (11)$$

whereas in the large ω limit, we find

$$\text{PSD}_z \sim \frac{k_B T}{3(4\eta^2\kappa)^{1/3}\omega^{5/3}} \quad (\omega \rightarrow \infty). \quad (12)$$

The expression in (12) suggests that the Z-power spectrum obeys a power-law decay at large frequencies ω , with an exponent $-5/3$.

Consider a birefringent particle stuck on the cell membrane, which is characterised by height fluctuations $h(\mathbf{r},t)$, where $\mathbf{r} = (x,y)$ are points on the plane of projection, which we define as the x - y plane.

The slope of the optic axis of the birefringent particle placed on the cell membrane (shown in Fig. 1) at a particular instant in the h - r plane is given by,

$$\tan(\theta) = \frac{h_2 - h_1}{r_2 - r_1} \quad (13)$$

where the particle touches the cell membrane between r_1 and r_2 , such that $r_2 - r_1$ is the length of the contact for the particle. This is of the order of 100 nm for a 1 μm diameter particle and is assumed to remain constant during rotational motion.

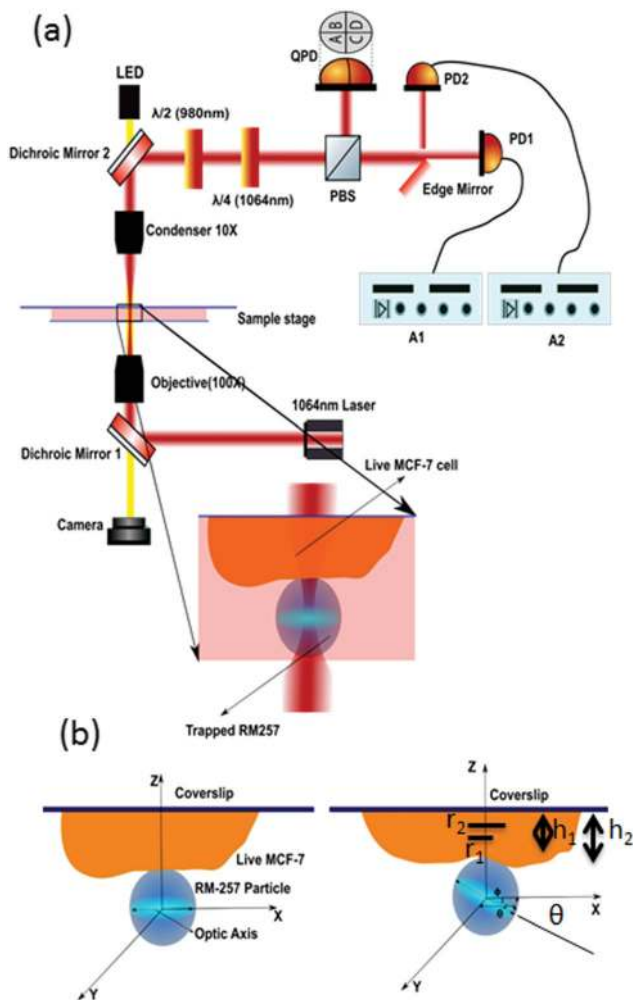


Fig. 1 (a) Schematic diagram of the set-up used to detect pitch rotation. A very well polarized 1064 nm laser beam is used to trap the particle, which then passes through into the forward scatter direction. The component of the forward scattered light orthogonal to the input polarization is sent into an edge mirror to ascertain the asymmetry in the scatter pattern. (b) The pitch rotation detection technique is used to find the local slope fluctuations of the cell membrane as shown in this cartoon.

For small angles θ , we may approximate $\tan \theta \approx \theta$. Within this approximation, the appropriate generalisation of (13) for the two-dimensional membrane surface is

$$\theta(\mathbf{r}, t) = \partial_r h(\mathbf{r}, t), \quad (14)$$

where \mathbf{r} is the location of the centre of the particle in the x - y plane. In terms of the Fourier transform $h_q(t)$, the angle θ becomes

$$\theta(\mathbf{r}, t) = -\frac{i}{(2\pi)^2} \int d^2 \mathbf{q} h_q(t) q \cos \phi e^{-i\mathbf{q} \cdot \mathbf{r}}, \quad (15)$$

where ϕ is the angle between the (fixed) vector \mathbf{r} and \mathbf{q} . After using the auto-correlation for the height field given in (6) and carrying out the angular integration, the auto-correlation of the angle becomes

$$\langle \theta(\mathbf{r}, 0) \theta(\mathbf{r}, t) \rangle = \frac{1}{4\pi} \int d^2 q q^3 F(q) e^{-\omega_q t} \quad (16)$$

where the function $F(q)$ has been given in (7). Upon substituting the latter in (16), and using the Wiener-Khinchin theorem, the PSD for the angle/slope fluctuations is found to have the general form

$$\text{PSD}_\theta = \frac{2\eta k_B T}{\pi} \int dq \frac{q^2}{(\kappa q^3 + \sigma q)^2 + (4\eta\omega)^2} \quad (17)$$

After a careful analysis of the integral, we find that the low frequency and high frequency behaviours of (17) are given by

$$\text{PSD}_\theta = \frac{8k_B T \eta}{3\pi \sqrt{\sigma^3 \kappa}} - \frac{4k_B T \eta^2}{\sigma^3} \omega \quad (\omega \rightarrow 0) \quad (18)$$

$$\text{PSD}_\theta = \frac{k_B T}{12\kappa\omega} \quad (\omega \rightarrow \infty) \quad (19)$$

Thus, we find the functional relationships for the PSD for pitch motion at low and high frequencies.

2 Experimental details

The experiment was performed using an optical tweezers kit OTKB/M (Thorlabs, USA) in an inverted configuration, where a linearly polarized 1.7 W, 1064 nm wavelength diode laser (Lasever, China) was used to form the optical tweezers. The objective was an Olympus 100 \times , 1.3 NA oil immersion one with the illumination aperture being overfilled and the condenser being a 10 \times , 0.25 NA Nikon air-immersion one. The power of laser light at the sample plane was set to be about 100 mW. The schematic diagram has been shown in Fig. 1. An LED lamp illuminates the sample from the top using a dichroic mirror, while another dichroic collects the visible light to be placed in a CMOS camera (Thorlabs). The forward scattered light emerges through the top dichroic and is sent into a polarizing beam splitter, where most of the light through one of the ports and sent into a Quadrant Photodiode (QPD). The other arm experiences a minimum in scattered intensity and experiences a complete dark when there are no particles in the trapping region.

The tracer particles that we used are birefringent liquid crystalline RM257 (Merck) particles made using standard techniques^{32,33} and of typical diameter $1 \pm 0.1 \mu\text{m}$. When these particles are trapped in optical tweezers, the birefringence axis aligns with that of the polarization of light, both in the conventional yaw and the pitch sense. When a well-linearly polarized light is used to trap a birefringent particle, some amount of light also emerges from the dark port of the polarizing beam splitter placed in the forward direction, due to the internal structure of the directors of the particle resulting in a four-lobe scatter intensity pattern. It has been shown in ref. 22 that the distribution of light in between these halves becomes anisotropic when the particle turns in the pitch sense. We exploit this very facet to ascertain the pitch motion.

We place an edge mirror in the path of the dark port of the polarizing beam splitter (PBS) in the forward direction and send one half of the scattered light into one photodiode (PD1),

while sending the other half to a different photodiode (PD2). These photodiode signals are amplified with current amplifiers and then sent into the Data Acquisition System (DAQ card, National Instruments) at a sampling rate of 40 kHz. These time series signals from PD1 and PD2 are then subtracted to gain the pitch signal. The advantage of using this configuration, as opposed to another QPD, is that larger gains can be obtained here.

If we look at the Fig. 1(a), we can notice a quarter wave-plate, in conjugation with a half wave-plate placed in the output path of the light after it escapes the sample chamber. A combination of these two can compensate for complicated shifts in phase due to the cell. We adjust these two such that the output of the polarizing beam splitter (PBS) which detects pitch motion has a good minimum in intensity (almost dark). Then we study the fluctuations of the intensity.

Typical *X*, *Z* and pitch power spectra for a birefringent particle trapped in water are shown in Fig. 2.

The *X* and *Z* PSD are the usual Lorentzian in nature, the pitch spectra is also found to be a good Lorentzian. This can be used for calibrating the pitch motion using eqn (1).²⁵ The pitch rotational trap stiffness k_1 is calculated from the eqn (2) and (4) is given by 1834 ± 600 pN nm rad⁻¹.

Michigan Cancer Foundation-7 (MCF-7) cells were grown on glass slides coated with gelatin. These slides were initially treated with the piranha solution and sterilized with a UV (265 nm) lamp for 20 minutes and thereafter coated with 0.5% gelatin solution. MCF7 cells were added towards the center of the coverslip and the Dulbecco's Modified Eagle Medium (DMEM) supplemented with 10% fetal bovine serum and 1% glutamine–penicillin–streptomycin was added on top of the coverslip. 10 μ L of birefringent sample with particles suspended in water was added to the cells. Cells were incubated at 5% carbondioxide and 37 °C.

One such birefringent particle was trapped and gradually brought in contact with the cell surface and held for about 10 seconds. It is well known that a birefringent particle aligns with the axis along the direction of linear polarization of the trapping beam both in the yaw sense and in the pitch sense.³² Thus, the particle automatically aligns in the preferred orientation while binding. It is then observed that the particle attaches to the cell by forming non-specific binding to present us with an excellent opportunity to probe the fluctuations of the cell membrane.³⁴ We simultaneously probe the slope fluctuations of the membrane from the light scattered by the birefringent particle while in contact with the membrane, as explained in eqn (18).

3 Results and discussions

The power spectral density of the motion of the particle normal to the membrane and the slope fluctuations are reported in Fig. 3.

The Fig. 3(a) indicates the PSD for the normal motion of the cell membrane. We find this to fit well to a power law with exponent $-5/3$,¹² particularly at high frequencies between 10 Hz

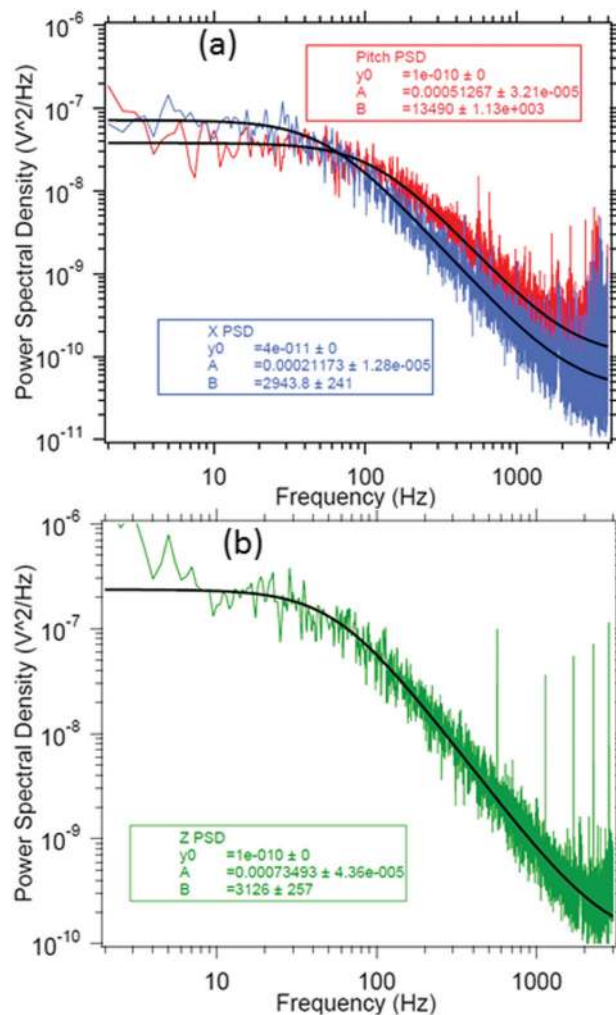


Fig. 2 The power spectra for (a) the pitch motion and the transverse *x* motion (b) for the axial *Z* motion, fitted to Lorentzians (eqn (1)) for calibration purposes.

and 1 kHz. This is consistent with the theory presented in eqn (12) for normal fluctuations, thereby indicating that the particle is indeed attached to the cell membrane and probing the normal fluctuations, not to mention this being also consistent with existent literature.³⁵ We simultaneously ascertain, for the same particle, the slope fluctuation PSD and show in Fig. 3(b). This PSD fits well to a power law and shows an exponent of 1.25 ± 0.16 , which we call the pitch PSD. Calibrating the pitch motion amplitude with factors from Fig. 2, we find ourselves capable of resolving 100 mdeg at 40 Hz. We also show the noise floor in Fig. 3(b) (green curve). The torque applied by the laser light on the particle is given as $1834 \times (\pi/180) \times 1.33 \times 0.1 = 4.2$ pN nm, considering a 0.1 degree angular rotation. The factor of 1.33 is due to the faxen correction given in eqn (4), for the particle placed very close to the surface. Now, the membranes fluctuate due to forces in excess of 5 to 10 pN.³⁶ Further, the particle has an attachment diameter of about 100 nm. Then the torque applied by the cell membrane onto the particle during the process of slope fluctuation is in excess of 500 to 1000 pN nm, which is at least an order of magnitude higher than the torque applied by the light onto the

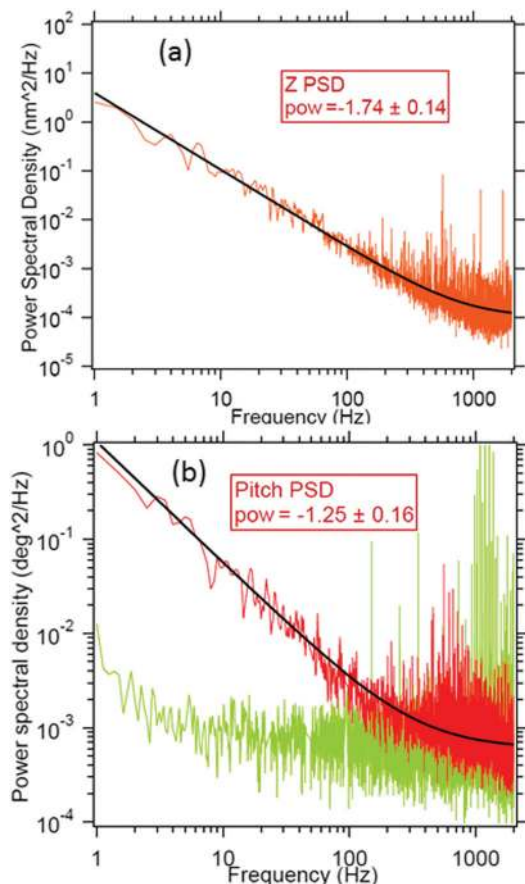


Fig. 3 The calibrated Power Spectral Densities (PSD) for (a) the normal fluctuations of the membrane (b) the local slope fluctuations of the membrane indicated by the Pitch angle, ascertained from the same particle simultaneously. In (b), the background PSD with the particle placed on a solid glass surface (without membrane fluctuations) is shown in green.

particle. Thus the effect of the optical torque on the system can be neglected. Moreover, the system is residing in a water based buffer medium, such that it is in an overdamped environment. Thus, the inertial terms are also negligible.

The power spectra shown in Fig. 3 have been fit to power laws of the form eqn (20).

$$\text{PSD} = Df^{\text{pow}}. \quad (20)$$

In the Fig. 3, where the power spectral densities for the normal fluctuations and the slope fluctuations have been shown, the spectra for the normal fluctuations yields a power law with exponent $-5/3$, which corresponds to the normal fluctuations for a free membrane. Thus, we may assume that, given the conditions are the same for the slope fluctuations too, the effect is only due to the membrane. Moreover, cytoskeletal effects can be induced by adding drugs like Latrunculin-B when the normal fluctuations shows a power law with spectra $-4/3$, and when the actin in the cytoskeleton depolymerizes to indicate membrane fluctuations in the proximity to a rigid wall. That is not the case here.

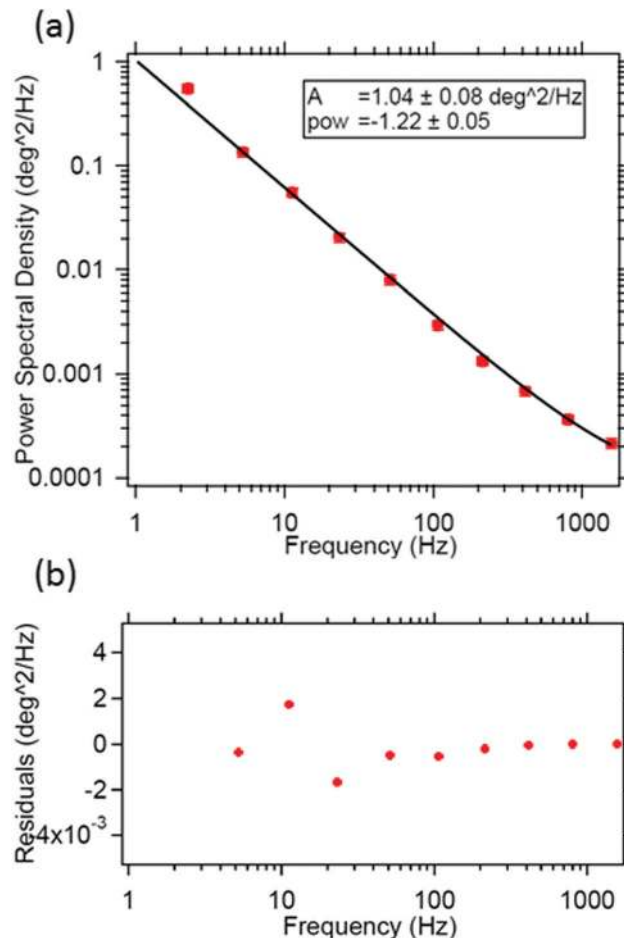


Fig. 4 (a) A typical pitch PSD data for a particle placed on the cell membrane is shown here. The data has been averaged in logarithmic blocks and then subsequently fitted to a power law. (b) The residuals are reported here. The data fits well to 5% error above 5 Hz but starts deviating as one goes lower than 5 Hz.

In order to ascertain the accuracy of the power law when fitted to the pitch PSD, we block average³⁷ the PSD data in exponents of 2 (namely 1, 2, 4, 8 and so on). This block averaged PSD also fits well to the power law, within 5% error, till about 5 Hz but starts deviating upon using lower frequencies, with the exponent being 1.22 ± 0.15 , as shown in Fig. 4. Here, the amplitude of the PSD at 40 Hz for a bandwidth of 1 Hz is $0.01 \text{ deg}^2 \text{ Hz}^{-1}$. Then the amplitude of the pitch motion is 0.1 deg over a bandwidth of 1 Hz.

We also show the statistics of pitch exponents observed in our experiments in Fig. 5. The average value of the pitch exponent is obtained to be -1.15 ± 0.12 . This exponent is comparable with the expected pitch exponent of -1 , as indicated in eqn (18), and consistent to a p -value of 0.0001.

We also show, in Fig. 6(a), that the value of the bending rigidity estimated from the measurement of the slope is coming to be $1.88 \pm 0.42 \times 10^{-19} \text{ J}$, which is consistent with literature values.¹³ The PSD in eqn (20) has been compared to eqn (19), such that $D = \frac{k_B T}{24\pi\kappa}$. Thus κ can be estimated.

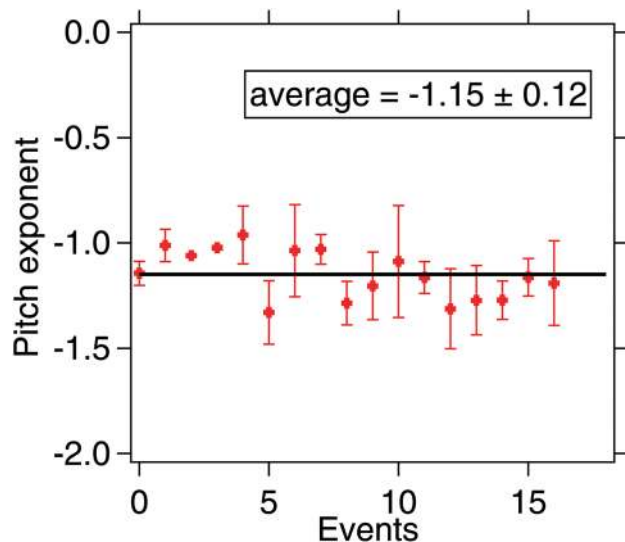


Fig. 5 The variation of pitch exponents for different measurement events. The average value of the exponent to the power law fit is -1.15 ± 0.12 , consistent to -1 with a p -value of 0.0001.

The curves for the normal and slope fluctuations can be simultaneously used to ascertain the bending rigidity, the cytoplasmic viscosity and the surface tension at high accuracy. We estimate the effective cytoplasmic viscosity from the eqn (12) and (19) and report the result in Fig. 6(b) with an average value 62.7 ± 15.6 Pa s. The viscosity is higher than expected for a cell cytoplasm,³⁸ but typically also involves the fluid getting trapped in the membrane, like reported by Biswas *et al.*¹³ Estimation of the membrane tension requires fits to the PSD at low frequencies, the regime where our laser intensity is not stable enough and hence does not yield meaningful results. Such experiment shall require complete redesign of the experimental setup, and beyond the scope of the present study.

There are reports in the literature about corrections to the eqn (12), on the basis of correction terms to the energy due to tilt-dependence.^{39,40} However, such theory yields a functional form for the PSD at high frequency that does not fit to the pitch PSD. This could be due to the curvature tilts at length-scales of 10 to 20 nm while the size of the birefringent particle being $1 \mu\text{m}$ with a base contact being of the order of 100 nm. Thus, such a probe cannot sample the bending to the membrane due to tilt-dependence.

The particle that has been used is a typically of $1 \mu\text{m}$ diameter and is well attached to the membrane by non-specific binding. The estimation of the normal fluctuations yields a power law with the amplitude and the exponent both matching well with previous experiments. Thus, we believe that the particle has negligible effect on the results obtained. In view of this, we used the pitch motion to study slope fluctuations of the cell membrane and then estimated the bending rigidity of the cell membrane from the coefficient to the power law fit. We find that the bending rigidity values obtained here are comparable to the values reported in literature. Thus, we do not deem it necessary to account for the presence of the particle on the membrane in the theory.

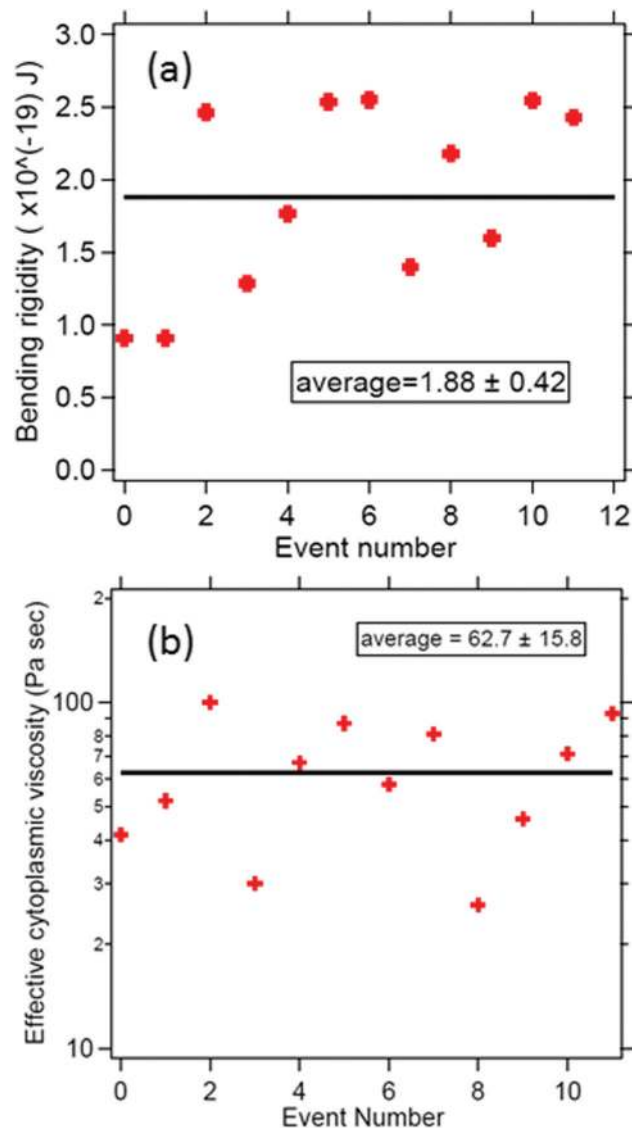


Fig. 6 This figure shows the variation of the calculated bending rigidity from the amplitudes of the power laws fitted to the high frequency region of the pitch PSD. The values are consistent with the values previously mentioned in the literature.

4 Conclusions

Thus to conclude, we have developed a new technique to ascertain the pitch rotational motion to a high sensitivity using optical tweezers. The pitch power spectrum for a birefringent particle trapped in water fits well to a Lorentzian. This particle can be attached non-specifically to a cell membrane by holding it against the membrane for 10 seconds. As soon as the particle attaches to the membrane, the vertical fluctuations of the particle can be used to find the membrane fluctuations. The PSD of the vertical fluctuations shows a power law exponent of $-5/3$, confirming that the particle is indeed recording the normal membrane fluctuations. We simultaneously ascertain the slope fluctuations of the membrane and find that the PSD fits well to a power law with the exponent consistent to -1 with

a p -value of 0.0001. The coefficient to the power law fit to the slope fluctuation PSD yields information about the cell membrane parameters like the bending rigidity and the effective cytoplasmic viscosity. This can be used to study the cell membrane to a better accuracy than previously possible with non-contact based techniques. Further, the fact that the measurement uses slope fluctuations raises the possibility of studying the vectorial nature of the cell membrane parameters. Such study is beyond the scope of the present manuscript.

Conflicts of interest

There are no conflicts to declare.

Acknowledgements

We thank the Indian Institute of Technology Madras for their seed and initiation grants. S. B. thanks Department of Science and Technology, Government of India for the grant YSS/2014/000523.

Notes and references

- J. T. Parsons, A. R. Horwitz and M. A. Schwartz, *Nat. Rev. Mol. Cell Biol.*, 2010, **11**, 633–643.
- T. Lecuit and P. F. Lenne, *Nat. Rev. Mol. Cell Biol.*, 2007, **8**, 633–644.
- H. T. McMahon and J. T. Gallop, *Nature*, 2005, **438**, 590–596.
- J. Kim, H. Jo, H. Hong, M. H. Kim, J. K. Lee, W. D. Heo and J. Kim, *Nat. Commun.*, 2015, **6**, 6781.
- Y. Park, M. Diez-Silva, G. Popescu, G. Lykotrafitis, W. Choi, M. S. Feld and S. Suresh, *Proc. Natl. Acad. Sci. U. S. A.*, 2008, **105**, 13730–13735.
- P. Connes, T. Alexy, J. Detterich, M. Romana, M.-D. Hardy-Dessources and S. K. Ballas, *Blood Rev.*, 2016, **30**, 111–118.
- D. Wirtz, K. Konstantopoulos and P. C. Searson, *Nat. Rev. Cancer*, 2011, **11**, 512–522.
- S. E. Winograd-Katz, R. Fassler, B. Geiger and K. R. Legate, *Nat. Rev. Mol. Cell Biol.*, 2014, **15**, 273–288.
- N. Gov, A. G. Zilman and S. Safran, *Phys. Rev. Lett.*, 2003, **90**, 228101.
- N. S. Gov and S. A. Safran, *Biophys. J.*, 2005, **88**, 1859–1874.
- Y. Park, C. A. Best, K. Badizadegan, R. R. Dasari, M. S. Feld, T. Kuriabova, M. L. Henle, A. J. Levine and G. Popescu, *Proc. Natl. Acad. Sci. U. S. A.*, 2010, **107**, 6731–6736.
- H. Yu, Y. Yang, Y. Yang, F. Zhang, S. Wang and N. Tao, *Nanoscale*, 2018, **10**, 5133–5139.
- A. Biswas, A. Alex and B. Sinha, *Biophys. J.*, 2017, **113**, 1768–1781.
- G. Giannone, B. J. Dubin-Thaler, H.-G. Dobreiner, N. Kieffer, A. R. Bresnick and M. P. Sheetz, *Cell*, 2004, **116**, 441–443.
- H.-G. Dobreiner, B. J. Dubin-Thaler, J. M. Hofman, H. S. Xenias, T. N. Sims, G. Giannone, M. L. Dustin, C. H. Wiggins and M. P. Sheetz, *Phys. Rev. Lett.*, 2006, **97**, 038102.
- C.-H. Chen, F.-C. Tsai, C.-C. Wang and C.-H. Lee, *Phys. Rev. Lett.*, 2009, **103**, 238101.
- C. Monzel, D. Schmidt, C. Kleusch, D. Kirchenbuchler, U. Seifert, A.-S. Smith, K. Sengupta and R. Merkel, *Nat. Commun.*, 2015, **6**, 8162.
- M. C. D. Santos, R. Deturche, C. Vezy and R. Jaffiol, *Biophys. J.*, 2016, **111**, 1316–1327.
- E.-L. Florin, A. Pralle, J. K. H. Horber and E. H. K. Stelzer, *J. Struct. Biol.*, 1997, **119**, 202–211.
- L. Friedrich and A. Rohrbach, *Nat. Nanotechnol.*, 2015, **10**, 1064–1069.
- F. Junger, F. Kohler, A. Meinel, T. Meyer, R. Nitschke, B. Erhard and A. Rohrbach, *Biophys. J.*, 2015, **109**, 869–882.
- B. Roy, A. Ramaiya and E. Schaffer, *J. Opt.*, 2018, **20**, 035603.
- J. Steinkuhler, E. Sezgin, I. Urbancic, C. Eggeling and R. Dimova, *Commun. Biol.*, 2019, **2**, 1–8.
- R. Dimova, *Adv. Colloid Interface Sci.*, 2014, **208**, 225–234.
- E. Schaffer, S. F. Norrelykke and J. Howard, *Langmuir*, 2007, **23**, 3654–3665.
- J. Leach, H. Mushfique, S. Keen, R. D. Leonardo, G. Ruocco, J. M. Cooper and M. J. Padgett, *Phys. Rev. E: Stat., Nonlinear, Soft Matter Phys.*, 2009, **79**, 026301.
- T. Betz and C. Sykes, *Soft Matter*, 2012, **8**, 5317–5326.
- T. Betz, M. Lenz, J. F. Joanny and C. Sykes, *Proc. Natl. Acad. Sci. U. S. A.*, 2009, **106**, 15320–15325.
- S. Ramaswamy, J. Toner and J. Prost, *Pramana*, 1999, **53**, 237–242.
- J. Prost, J.-B. Manneville and R. Bruinsma, *Eur. Phys. J. B*, 1998, **1**, 465–480.
- U. Siefert, *Phys. Rev. E: Stat., Nonlinear, Soft Matter Phys.*, 1994, **49**, 3124–3127.
- A. Ramaiya, B. Roy, M. Bugiel and E. Schaffer, *Proc. Natl. Acad. Sci. U. S. A.*, 2017, **114**, 10894–10899.
- R. Vaippully, D. Bhatt, A. D. Ranjan and B. Roy, *Phys. Scr.*, 2019, **94**, 105008.
- R. Vaippully, V. Ramanujan, S. Bajpai and B. Roy, *J. Phys.: Condens. Matter*, 2020, **32**, 235101.
- E. Helfer, S. Harlepp, L. Bourdieu, J. Robert, F. C. MacKintosh and D. Chatenay, *Phys. Rev. E: Stat., Nonlinear, Soft Matter Phys.*, 2001, **63**, 021904.
- K. Liu, B. Chu, J. Newby, E. L. Read, J. Lowengrub and J. Allard, *PLoS Comput. Biol.*, 2019, **15**, e1006352.
- K. Berg-Sorensen and H. Flyvbjerg, *Rev. Sci. Instrum.*, 2004, **75**, 594–612.
- R. Vaippully, V. Ramanujan, S. Bajpai and B. Roy, *J. Phys.: Condens. Matter*, 2020, **32**, 235101.
- M. S. Jablin, K. Akabori and J. F. Nagle, *Phys. Rev. Lett.*, 2014, **113**, 248102.
- J. F. Nagle, M. S. Jablin, S. Tristram-Nagle and K. Akabori, *Chem. Phys. Lipids*, 2015, **185**, 3–10.